Supplemental Material:

Figure S1:

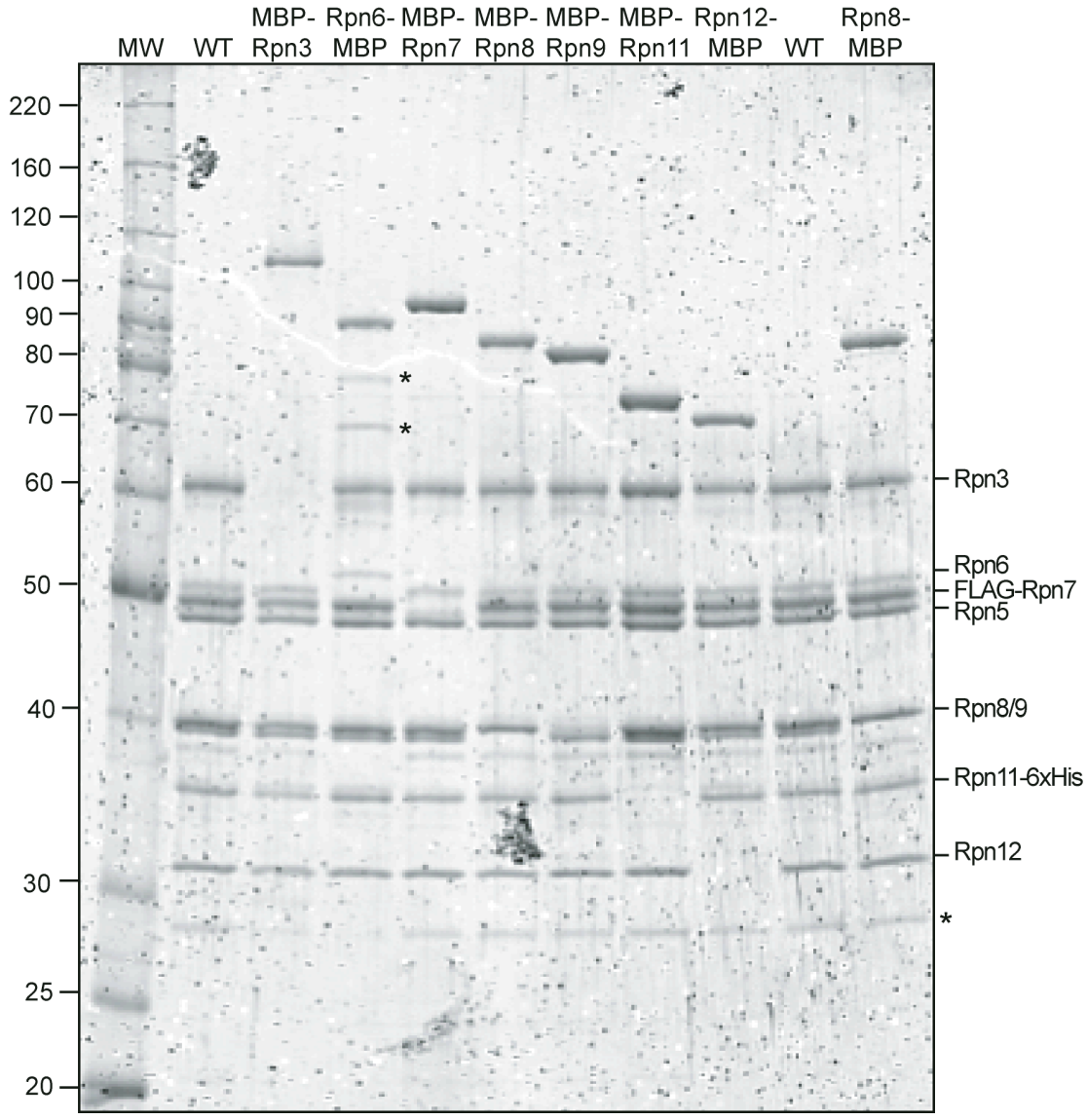

Wild-type and MBP-fused recombinant lid. Sypro Ruby-stained SDS-PAGE gel showing purified recombinant lid with MBP-fused to the N- or C-terminus of individual subunits as indicated. Fused subunits are shifted relative to their wild-type counterpart. * denotes minor degradation products.

Rpn6-MBP migrates at lower molecular weight than expected based on the untagged protein. This anomalous behavior might be a consequence of the MBP fusion or caused by proteolytic cleavage of the N-terminus of Rpn6. Class averages of recombinant lid display this N-terminal Rpn6 truncation. To select for lid subcomplexes with full-length Rpn6, the FLAG tag was transferred from Rpn7 to the N-terminus of Rpn6 (see supplemental methods and Fig. S8).

Figure S2:

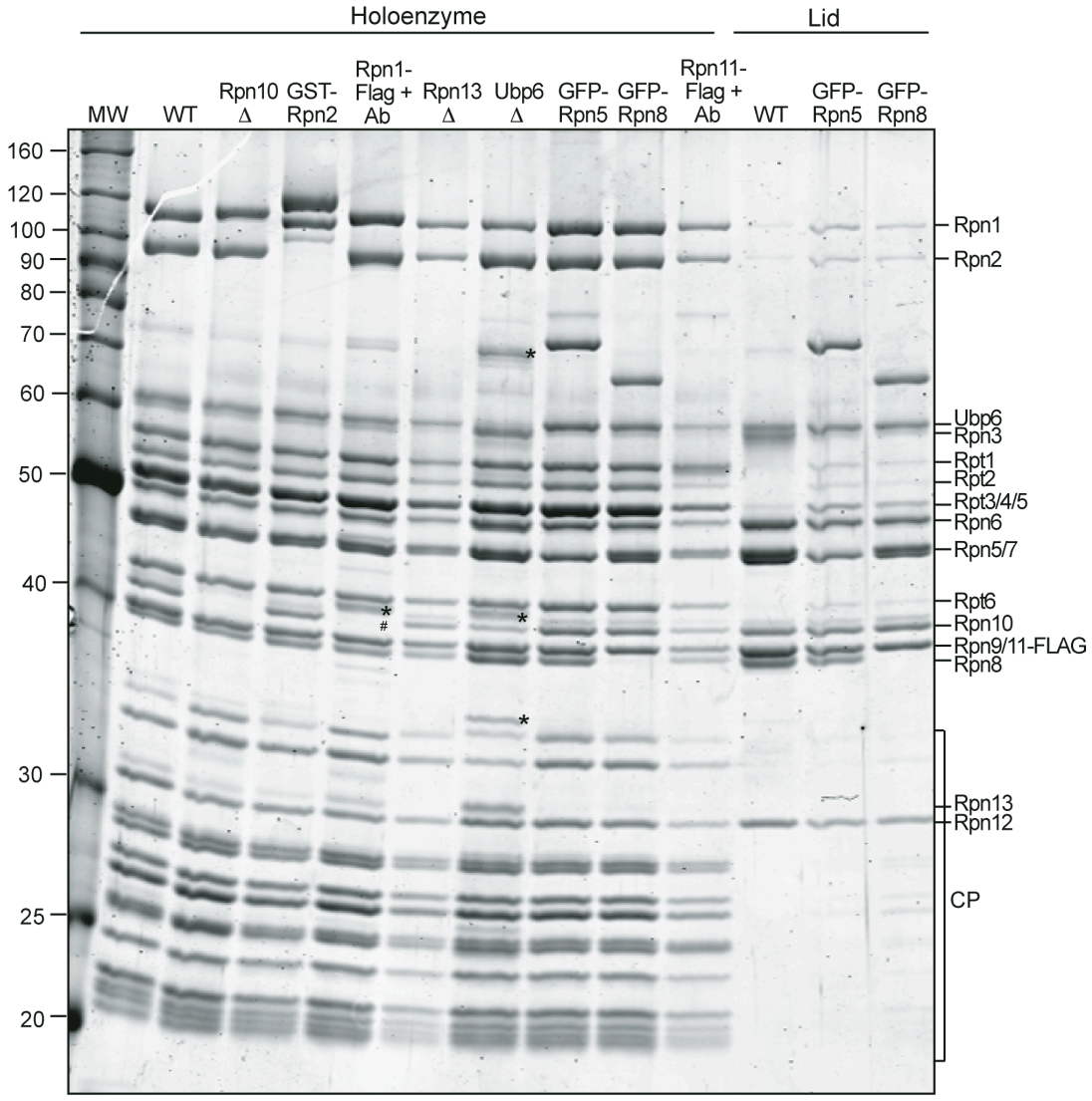

Purified endogenous holoenzyme and lid used in EM analyses. Holoenzyme or lid was purified from yeast strains containing the indicated tag or deletions and a FLAG tag on Rpn11 (with the exception of Rpn1-FLAG) as described, separated by SDS PAGE, and stained with Sypro Ruby. +Ab indicates that sample was incubated with anti-FLAG antibody and purified by gel filtration. * indicates more prominent background bands. # indicates the loss of Rpn10 from Rpn1-FLAG holoenzyme after incubation with anti-FLAG antibody.

Figure S3:

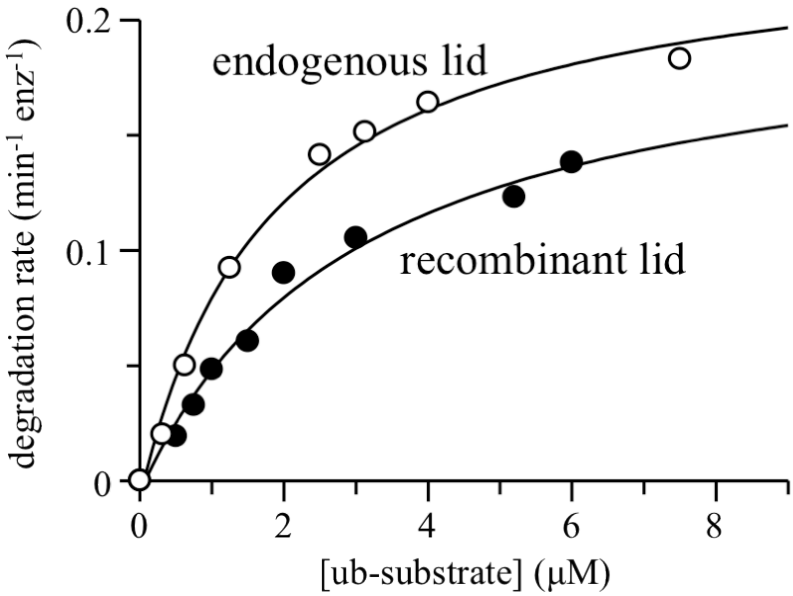

Michaelis-Menten analyses for substrate degradation by holoenzymes reconstituted with recombinant and endogenous lid. Ubiquitinated GFP-titin-cyclin fusion substrate was degraded at 30 °C by proteasome holoenzyme (200 nM) reconstituted from base, 20S core, and recombinant or endogenous lid. Values for K_M and v_{max} were 1.8 μM and 0.24 min^{-1} enz^{-1} for holoenzyme with endogenous lid, and 3.0 μM and 0.21 min^{-1} enz^{-1} for holoenzyme with recombinant lid. The lack of post-translational modifications in *E. coli* might account for these differences.

Figure S4:

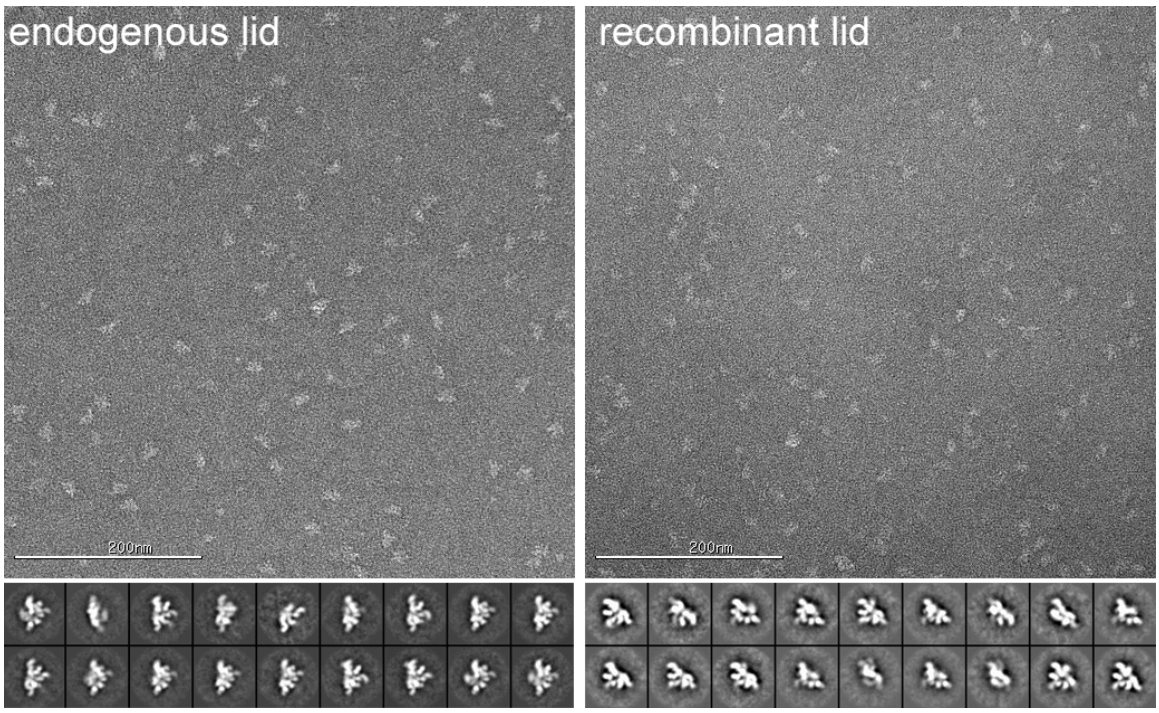

Micrographs of negatively stained endogenous (left) and recombinantly expressed (right) yeast lid subcomplexes. Corresponding 2D class averages of the particles are shown directly below the micrograph, demonstrating that the recombinant lid exhibits the same overall morphology as the endogenous.

Figure S5:

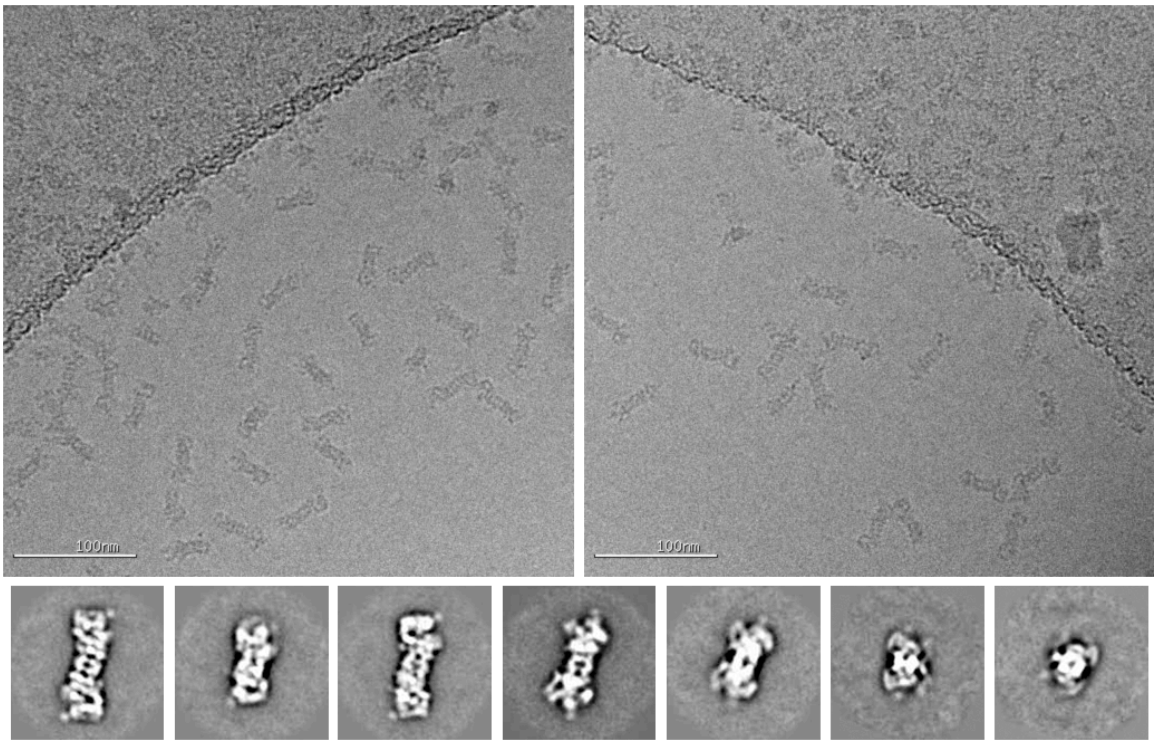

Proteasome holoenzymes preserved in a frozen-hydrated state. Proteasome particles can be observed adopting a range of orientations, even a vertical position, when imaged through thick ice. Reference-free 2D class averages (beneath the micrographs) show a variety of views.

Figure S6:

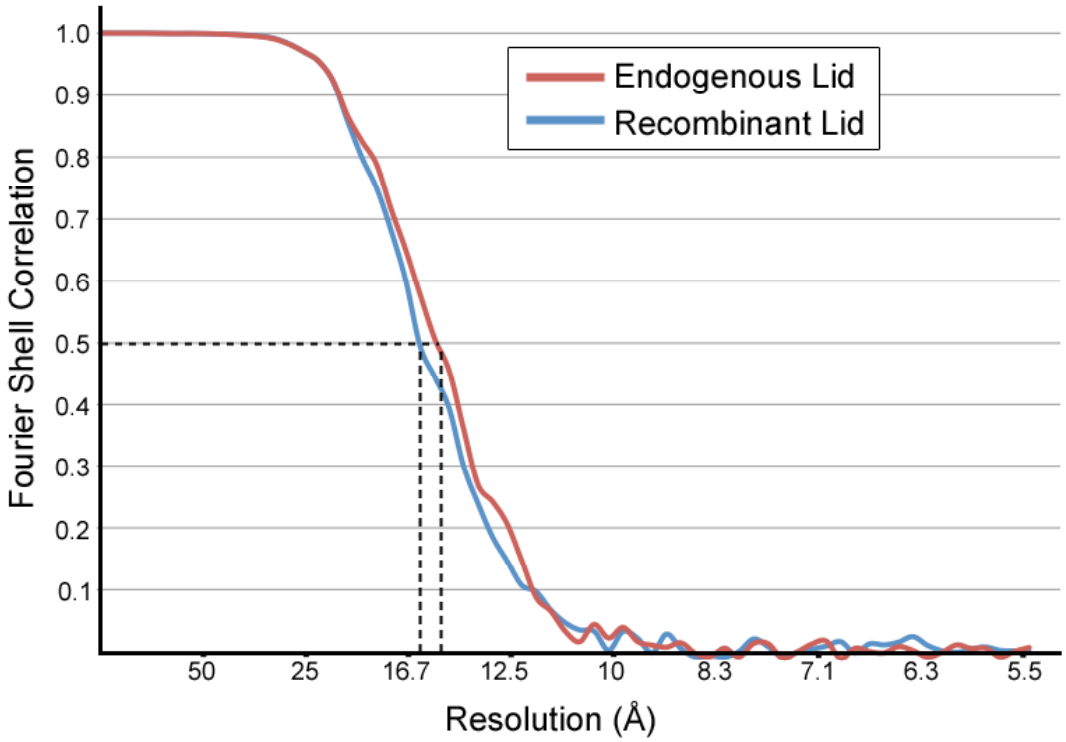

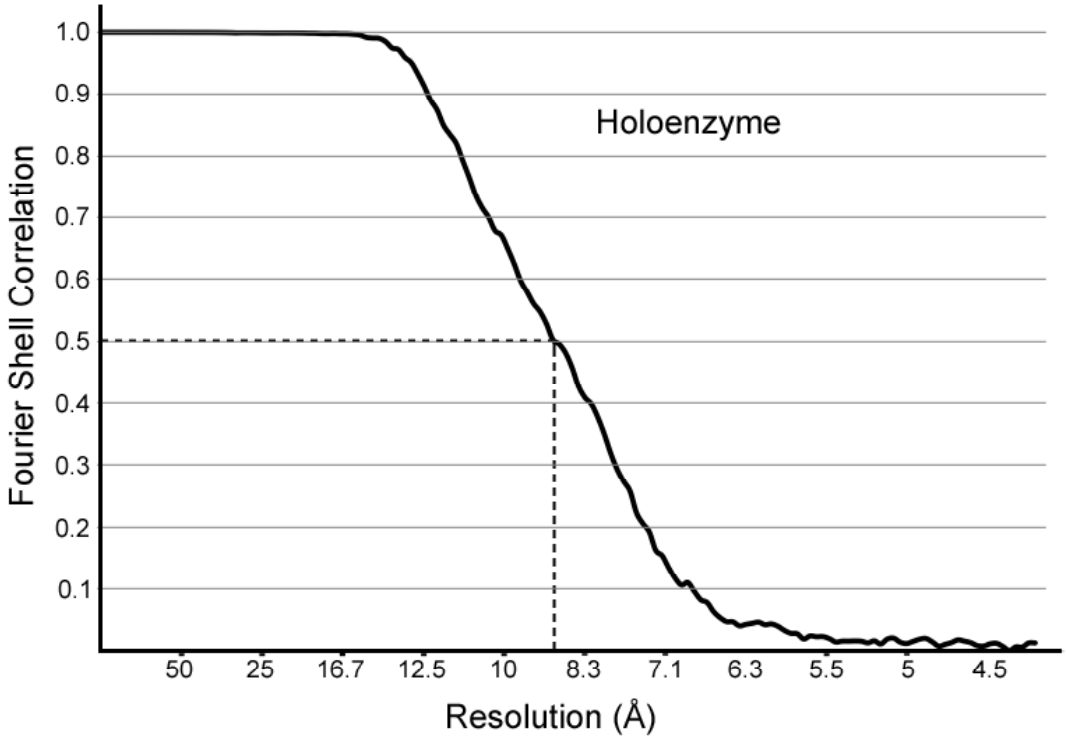

Estimated resolutions. Resolutions of the reconstructions were estimated using a Fourier shell correlation of back projected even/odd datasets, using a criterion of 0.5 correlation. Reported resolutions for the endogenous and recombinant negative stain lid structures are 15 Å and 16 Å, respectively. The resolution for the cryoEM reconstruction is estimated to be 8.8 Å.

Figure S7:

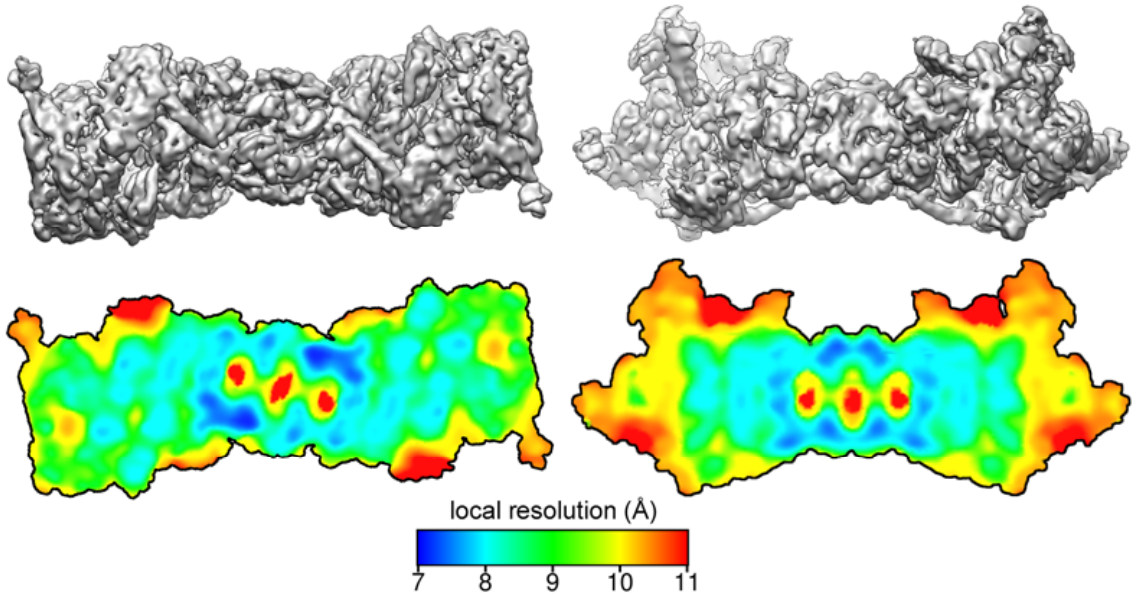

Local resolution map of the holoenzyme cryoEM density. A local resolution calculation of the proteasome reconstruction shows a range of resolutions within the map. In grey are surface representations of the reconstruction, and shown below are cross-sections through the center of the density. The cross sections are colored according the map's calculated local resolution, with the highest resolution portions in dark blue, and the lowest resolution areas in red. Notably, the core particle and AAA+ ATPases contain the highest resolution data, and the ubiquitin receptors are the lowest in resolution.

Figure S8:

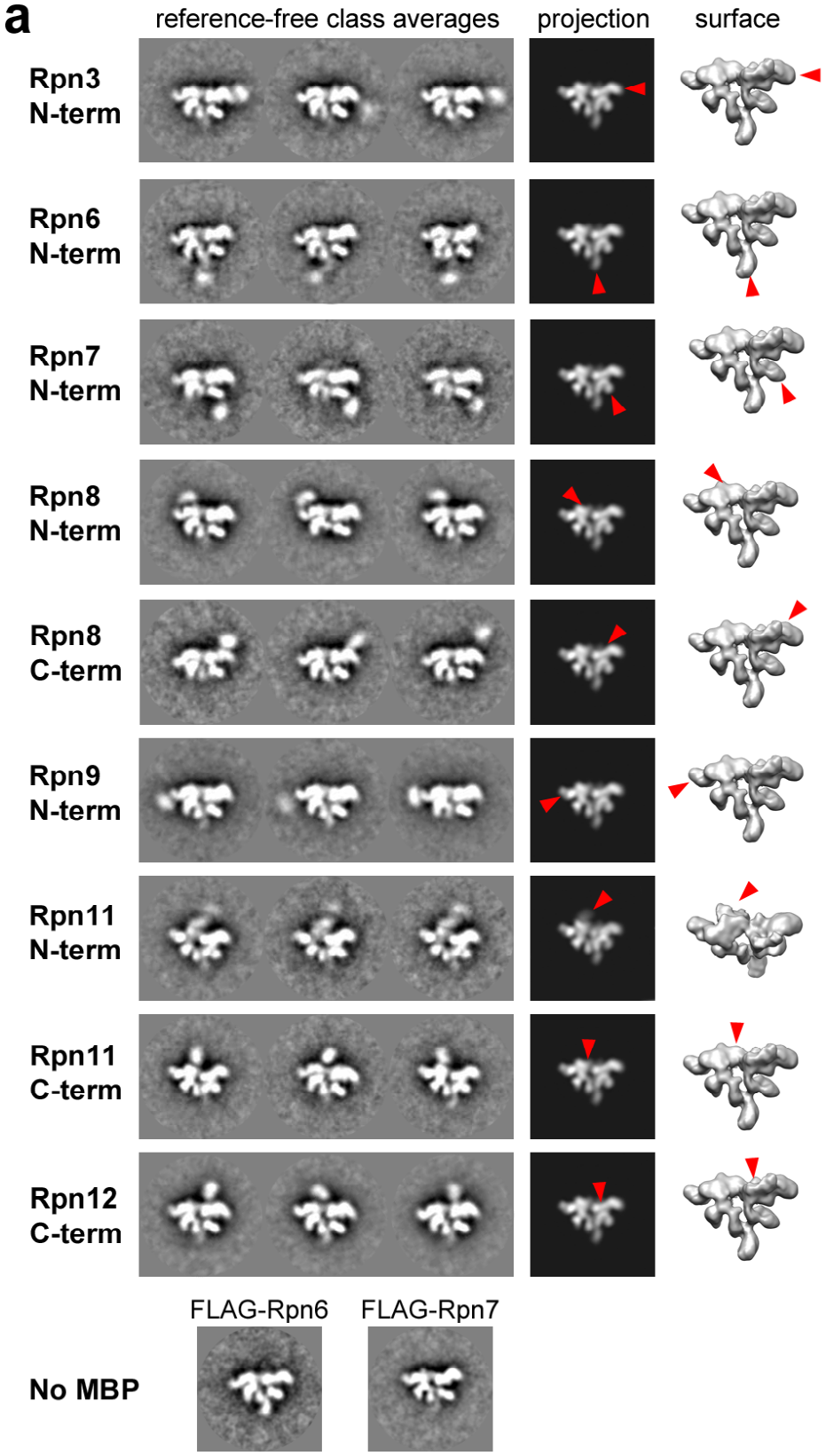
a
reference-free class averages
projection
surface
Rpn3 N-term
Rpn6 N-term
Rpn7 N-term
Rpn8 N-term
Rpn8 C-term
Rpn9 N-term
Rpn11 N-term
Rpn11 C-term
Rpn12 C-term
FLAG-Rpn6
FLAG-Rpn7
No MBP

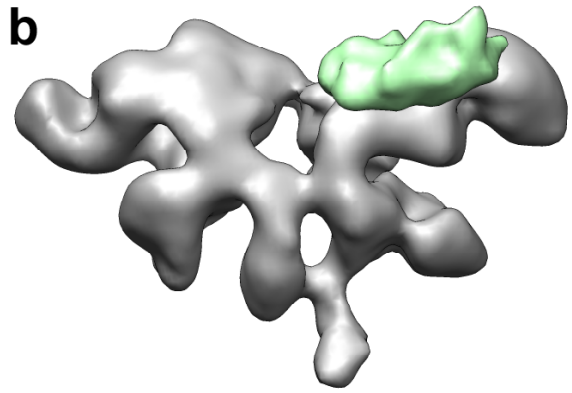

Localization of lid subcomplex subunits by MBP labeling. a) Constructs bearing a FLAG tag on RPN7 and an MBP tag at either the N- or C-terminus of specific subunits were recombinantly expressed in *E. coli* and purified for EM analysis. MBP tags can be clearly observed as a small bright density attached to the subcomplex in reference-free 2D class averages. Three representative class averages for each of the analyzed constructs are shown in the leftmost column. Each MBP tag was unmistakably identifiable in the canonical front view of the lid particles, with the exception of the N-terminal Rpn11, which was only visible in a tilted view of the particle. The corresponding forward projection and surface representation of the recombinant lid reconstruction is shown to the right of each set of class averages, indicating the subunit localization with a red arrowhead. Notably, we see decreased density for the N-terminal portions of Rpn6, which is caused by a fraction of particles with N-terminal Rpn6 truncations (see also Fig. S1). We were able to select for a full-length Rpn6 by purifying the complex using a FLAG tag on Rpn6 (bottom panel) b) A Rpn12-deletion mutant clearly shows the location of Rpn12 in the lid complex. The difference density between the recombinant lid and recombinant Rpn12 delete lid is shown in green.

Figure S9:

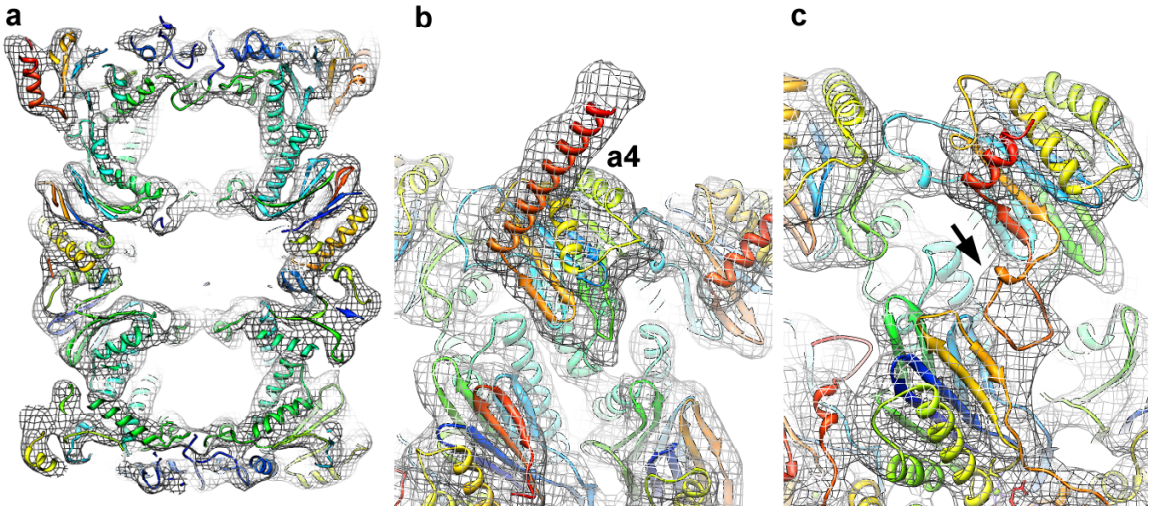

Unambiguous docking of the crystal structure for yeast 20S core. Docking of the 20S core structure (PDBid: 1ryp) into the EM density provides an asymmetric orientation of the core relative to the base. a) Cross section of the crystal structure docked into the EM density, showing the high level of correlation between the molecular envelope of the electron density and the secondary structural elements of the atomic coordinates. b) Extended α-helix of the α4 subunit. The helix was extended to include the entire C-terminus. c) The insertion-loop of subunit α2 is obvious in the EM density.

Figure S10:

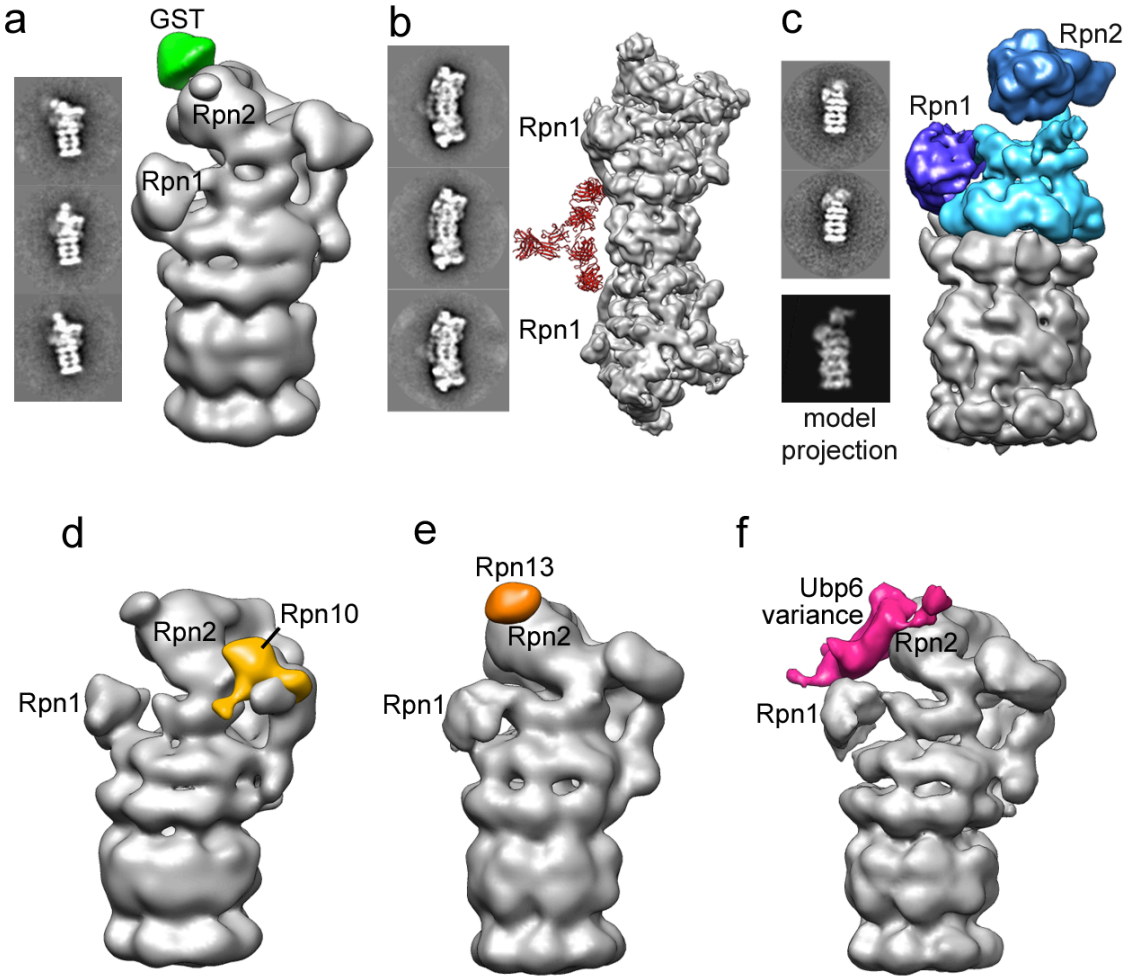

Localization of Rpn1, Rpn2, and ubiquitin-interacting subunits. a) Reference-free class averages and reconstruction of an N-terminal GST fusion of Rpn2 revealed its location on the top of the holoenzyme. b) Antibody labeling of a C-terminal Rpn1 FLAG tag results in 2D class averages showing a dimeric antibody with the single-chain variable fragments attached to Rpn1. The view observed in the class averages is depicted using the holoenzyme reconstruction, with an antibody modeled alongside it. c) A small subset of all holoenzyme preparations resulted in particles that had lost the lid subcomplex. Although there were not sufficient views of these aberrant particles to generate a 3D reconstruction, a theoretical model generated by including only Rpn1, Rpn2, Rpt1-6, and core particle subunits accurately represents the observed class averages (shown as forward projection and surface rendering). d, e) Deletion mutants were used to generate difference maps (colored) that indicate the locations of the ubiquitin receptors Rpn10 and Rpn13, respectively. f) Due to the variability of Ubp6, this DUB was localized by subtracting the variance map of the wild-type holoenzyme from a variance map of an Ubp6-deletion mutant. Difference variance map is colored magenta.

Figure S11:

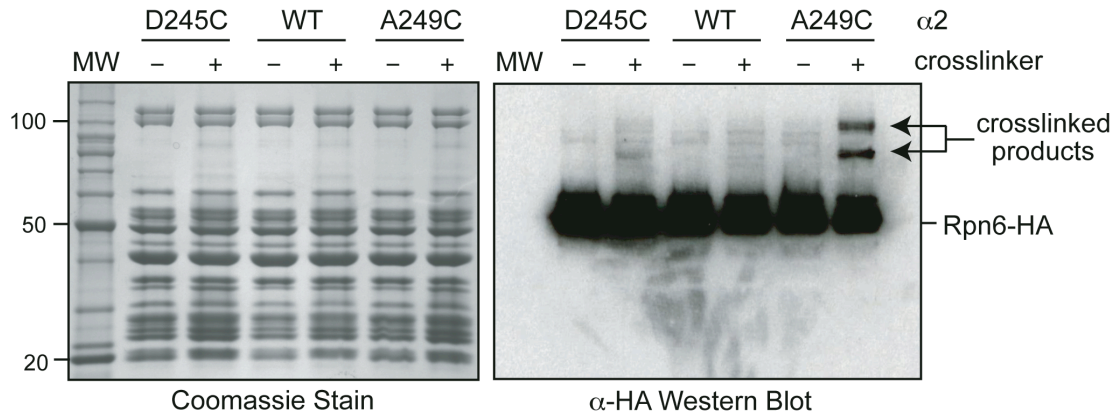

Rpn6 contacts subunit α2 of the 20S core. Our cryoEM reconstruction of the proteasome indicates a direct contact between the α2 subunit of the core particle and Rpn6 of the lid. To confirm this contact by crosslinking, we engineered a cysteine in α2 either at the predicted point of contact (A249C) or nearby (D245C), and conjugated sulfo-MBS, a short (7.3Å spacer arm) heterobifunctional crosslinker, to this site. The core particle contains other cysteines, but those are relatively inaccessible to cysteine-reactive modifying agents (data not shown). Crosslinker-conjugated (or mock-conjugated) core particle purified from strains containing WT, A249C, and D245C α2 was incubated with purified base, Rpn10, 0.5 mM ATP, and lid purified from a yeast strain in which Rpn6 was C-terminally tagged with a 3x hemagglutinin (HA) tag. Reactions were divided equally for separation by SDS-PAGE followed by either coomassie staining or anti-HA western blotting. Rpn6 has a molecular weight of 50 kDa, α2 of 27 kDa, and a crosslink between them should create an anti-HA-reactive band above 77 kDa. This crosslinked band appears only when the cysteine is placed at A249C, closest to the predicted contact between α2 and Rpn6. The two different crosslinked products likely represent crosslinking to two different sites on Rpn6.

Table S1. Strain List

Strain	Genotype	Source
YYS40	*MAT***a** *ade2-1 his3-11,15 leu2-3,112 trp1-1 ura3-1 can1 RPN11::RPN11-3XFLAG(HIS3)*	Y. Saeki
DOM90 (AFS92)	*MAT***a** *ade2-1 his3-11 leu2-3,112 trp1-1 ura3-1 can1-100 bar1*	A. Straight
RJD1144	*MAT***a** *his3Δ200 leu2-3,112 lys2-801 trpΔ63 ura3-52 PRE1-FLAG-6xHIS::Ylplac211*(*URA3*)	R. Deshaies
yAM1	*MAT***a** *ade2-1 his3-11,15 leu2-3,112 trp1-1 ura3-1 can1 RPN11::RPN11-3XFLAG(HIS3) rpn10Δ::KanMX*	This study
yAM2	*MAT***a** *ade2-1 his3-11,15 leu2-3,112 trp1-1 ura3-1 can1 RPN11::RPN11-3XFLAG(HIS3) rpn13Δ::KanMX*	This study
yAM3	*MAT***a** *ade2-1 his3-11,15 leu2-3,112 trp1-1 ura3-1 can1 RPN11::RPN11-3XFLAG(HIS3) ubp6Δ::KanMX*	This study
yAM4	*MAT***a** *ade2-1 his3-11,15 leu2-3,112 trp1-1 ura3-1 can1 RPN11::RPN11-3XFLAG(HIS3) KanMX-GAL1-GST-RPN2*	This study
yAM5	*MAT***a** *ade2-1 his3-11,15 leu2-3,112 trp1-1 ura3-1 can1 RPN11::RPN11-3XFLAG(HIS3) KanMX-GAL1-GFP-RPN5*	This study
yAM6	*MAT***a** *ade2-1 his3-11,15 leu2-3,112 trp1-1 ura3-1 can1 RPN11::RPN11-3XFLAG(HIS3) KanMX-GA1L-GFP-RPN8*	This study
yAM7	*MAT***a** *ade2-1 his3-11 leu2-3,112 trp1-1 ura3-1 can1-100 bar1 RPN1-FLAG-KanMX*	This study
yAM8	*MAT***a** *his3Λ200 leu2-3,112::P_{PRE8}-pre8A249C-LEU2 lys2-801 trpΔ63 ura3-52 PRE1-FLAG-6xHIS::Ylplac211*(*URA3*) *pre8Δ::KanMX*	This study
yAM9	*MAT***a** *his3Δ200 leu2-3,112::P_{PRE8}-pre8D245C-LEU2 lys2-801 trpΔ63 ura3-52 PRE1-FLAG-6xHIS::Ylplac211*(*URA3*) *pre8Δ::KanMX*	This study
yAM10	*MAT***a** *ade2-1 his3-11,15 leu2-3,112 trp1-1 ura3-1 can1 RPN11::RPN11-3XFLAG(HIS3) RPN6-3XHA-KanMX*	This study

Yeast strains used in the current study.